Research Article

Magnetic Resonance in Chemistry

Received: 13 December 2011 Revised: 14 February 2012 Accepted: 15 February 2012 Published online in Wiley Online Library

(wileyonlinelibrary.com) DOI 10.1002/mrc.3810

^{13}C GIAO DFT calculation as a tool for configuration prediction of N–O group in saturated heterocyclic *N*-oxides

Radek Pohl,[a] Francisc Potmischil,[b] Martin Dračínský,[a] Václav Vaněk,[a] Lenka Slavětínská[a] and Miloš Buděšínský[a]*

Tropane, tropinone, pseudopelletierine and cocaine were oxidized *in situ* in a nuclear magnetic resonance (NMR) tube providing mixtures of *exo*/*endo* *N*-oxides. Observed ^{13}C chemical shifts were correlated with values calculated by gauge-including atomic orbitals density functional theory (DFT) OPBE/6-31G* method using DFT B3LYP/6-31G* optimized geometries. The same method of ^{13}C chemical shift calculation was applied on series of methyl-substituted 1-methylpiperidines and their epimeric *N*-oxides described in literature. The results show that using this undemanding calculation method enables assignment of configuration of N–O group in *N*-epimeric saturated heterocyclic *N*-oxides. The approach enables assigning of the configuration with high degree of certainty even if NMR data of only one isomer are available. An improved method of *in situ* oxidation of starting amines in an NMR tube is also described. Copyright © 2012 John Wiley & Sons, Ltd.

Supporting information may be found in the online version of this article.

Keywords: NMR; ^{13}C; ^{1}H; saturated heterocyclic *N*-oxides; chemical shift calculations; DFT

Introduction

There is no doubt that the stereochemistry of a compound predefines its molecular properties such as reactivity or biological activity. Therefore, the assignment of the configuration is one of the key steps of the structure elucidation. There are several nuclear magnetic resonance (NMR) methods enabling relative configuration determination. Classical approach is employing of nuclear Overhauser effects (NOEs)[1] of spatially closed nuclei and/or Karplus relationship[2] between vicinal coupling constant and torsion angle of interacting nuclei. When a molecule motion tends to form several conformers in a fast equilibrium, then observed NMR parameters (NOE and ^{3}J) are averaged, which complicates decoding of stereochemical information. In this case, residual dipolar coupling methods have been found useful for flexible molecules.[3]

Another approach, which has become attractive in the last two decades, is a correlation of calculated NMR parameters with observed ones.[4] In combination with the probability calculation, this approach seems to be powerful even in the cases when NMR data of only one diastereoisomer are available.[5] When experimental NMR tools do not provide reliable assignment, the NMR parameters calculation is a method of choice as we showed in the case of chiral sulfoxides.[6]

Chiral *N*-oxides of tertiary amines bearing different substituents on the nitrogen atom resemble to some extent the structure of chiral sulfoxides where central chirality is manifested on the heteroatom.

Examples of chiral *N*-oxides are found in nature as various classes of alkaloids isolated from natural sources, e.g. (+)-bulbocapnine-β-*N*-oxide[7] from *Glaucium fimbrilligerum*, (+)-5,17-dehydromatrine *N*-oxide[8] from *Euchresta japonica*, pericine *N*-oxide[9] from *Kopsia arborea* and (4*S*)-corynoxeine *N*-oxide[10] from *Uncaria rhynchophylla*. Representatives of tropane *N*-oxide alkaloids have been also found in nature, e.g. 3α-tigloyloxytropane *N*-oxide[11] from *Physalis alkekengi*, darlingine *N*-oxide[12] from *Darlingia darlingiana*, catuabine E *N*-oxide[13] from *Erythroxylum vacciniifolium*, (+)-anhydroecgoine methyl ester *N*-oxide[14] from *Erythroxylum emarginatum*, astrmalvine A *N*-oxide[15] from *Astripomoea malvacea*, 7α-hydroxycatuabine H *N*-oxide and vaccinine B *N*-oxide[16] from *E. vacciniifolium* Mart. (Erythroxylaceae). Chiral *N*-oxides have found application in asymmetric catalysis, e.g. in asymmetric cyanosilylation of ketones,[17] in borane-mediated reduction of ketones[18] or in asymmetric allylation of aldehydes.[17]

The reports dealing with the configuration determination of chiral *N*-oxides by NMR spectroscopy are mainly based on NOE contacts of alkyl substituents on the nitrogen atom with other parts of the molecule.[7,19–22] The $^{1}J_{C,C}$ coupling constants were also used for the discrimination of *N*-epimeric amine oxides.[23] In addition to that, the *N*-oxide configuration has been successfully established using predicted ^{13}C chemical shifts according to the multilinear regression analysis of chemical shifts differences of amine oxides and parent amines.[24] The effect of N-oxidation of tertiary amines on ^{15}N chemical shifts was published as well

* *Correspondence to: Miloš Buděšínský, Institute of Organic Chemistry and Biochemistry, Academy of Science of the Czech Republic, Flemingovo nám. 2, CZ-166 10 Prague 6, Czech Republic. E-mail: budesinsky@uochb.cas.cz*

a *Institute of Organic Chemistry and Biochemistry, Academy of Science of the Czech Republic, Flemingovo nám. 2, CZ-166 10 Prague 6, Czech Republic*

b *Department of Organic Chemistry, Biochemistry and Catalysis, University of Bucharest, Bulev. Regina Elisabeta 4-12, RO-030018 Bucharest-1, Romania*

with conclusion that ^{15}N NMR cannot be used for configuration determination of *N*-oxides because of small chemical shift difference range.[25] On the other hand, ^{17}O NMR was found to be sensitive towards configuration of *N*-oxide[26] despite the fact that experimental data are accessible with difficulty.

Indispensable conditions for obtaining satisfactory correlation of calculated and observed chemical shifts are reproducibility and reliability of experimental data. We have found that experimental chemical shifts of amine *N*-oxides depend on the concentration of an acid in $CDCl_3$ because an equilibrium between protonized and free form of *N*-oxide exists (refer to the Results and Discussion section). Therefore, reproducible experimental data are obtained when the acid is neutralized. This omission led to incorrect experimental chemical shifts of model compounds in our previous paper.[29] Hence, the corrected experimental NMR data together with improved experimental procedure providing reproducible values are described in the present work. In addition, we would like to show that gauge-including atomic orbitals density functional theory (GIAO DFT) calculated ^{13}C chemical shifts can be used for *endo/exo* configuration determination of N–O group in tropane *N*-oxide derivatives **1a–4a** (*endo* N–O configuration, Fig. 1) and **1b–4b** (*exo* N–O configuration, Fig. 1). The *N*-oxides were prepared by *in situ* oxidation of parent tropane derivatives **1–4** in an NMR tube by using *m*-chloroperbenzoic acid (MCPBA) with subsequent neutralization by triethylamine (Et_3N).

Experimental

Amines **1–9**, $CDCl_3$, MCPBA, triethylamine (Et_3N), $CDCl_3$ and 4-methylmorpholine *N*-oxide **9a** used in this work were obtained commercially from Sigma-Aldrich Co. $CDCl_3$ was passed through a pad of basic alumina prior to use.

Amine *N*-oxides **1a–9a** were prepared by an *in situ* oxidation as follows: 0.05 mmol corresponding amines **1–9** were dissolved in 0.5 ml of $CDCl_3$. ^1H and ^{13}C NMR spectra of the amines were recorded, and the amine solutions were *in situ* oxidized with 1.5 Eq of MCPBA in an NMR tube. The oxidation is instant reaction and can be followed by NMR. The solution was then neutralized by addition of 6 Eq of Et_3N providing *N*-oxides **5a–9a** and mixtures of *exo/endo N*-oxides **1a–4a** and **1b–4b**.

The NMR spectra were measured on a Bruker Avance II 600 (with ^1H at 600.13 MHz and ^{13}C at 150.9 MHz frequency) using a 5 mm TXI cryo-probe or Bruker Avance II 500 (with ^1H at 499.8 MHz and ^{13}C at 125.7 MHz frequency) using a 5 mm TBO probe. The chemical shifts are given in δ-scale (with the ^1H shifts referenced to tetramethylsilane (TMS) and the ^{13}C shifts referenced to $CDCl_3$ using $\delta(CDCl_3) = 77.00$ ppm). The 2D homonuclear (H,H-COSY and H,H-ROESY) and 2D heteronuclear (H,C-HSQC and H,C-HMBC) experiments were performed when needed for the structural assignments of the signals (with standard 2D NMR pulse sequences of Bruker software being used).

The geometry optimizations and chemical shift calculations were performed using the Gaussian 09 software package (Gaussian, Inc., Wallingford CT, USA).[27] The molecular geometries were optimized at the B3LYP/6-31G* level of theory *in vacuum*. The conformation analysis of model compounds was performed in our previous paper,[29] and all calculated NMR data presented here are weighted averaged values according to the conformer population. The nuclear magnetic shielding constants were calculated by GIAO DFT using the OPBE/6-31 G* functional[28] basis set setup. Calculated chemical shifts were referenced to

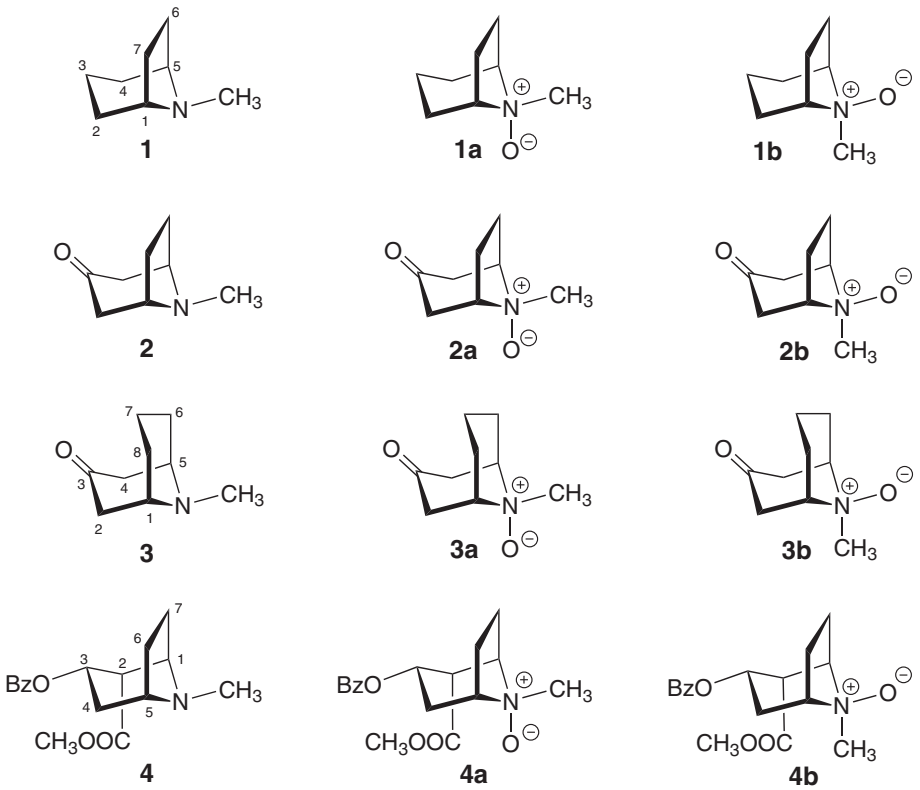

Figure 1. Tropane alkaloids **1–4** and corresponding *N*-oxides **1a–4a** and **1b–4b** studied in this work.

TMS (δ_{ref}(H) = 0 ppm, δ_{ref}(C) = 0 ppm) calculated at the same level of theory (nuclear shielding constants: σ(H) = 32.05, σ(C) = 194.06).

Results and Discussion

In our previous contribution,[29] we screened the computation methods on model amines **5–9** and amine oxides **5a–9a** (Fig. 2). The observed NMR data of amine oxides were measured after *in situ* oxidation, in $CDCl_3$ solution, of the parent amines with MCPBA in an NMR tube. Unfortunately, there, we have not taken into account that N-oxidation of the amines with MCPBA leads to the fast equilibrium mixture of amine oxides and *m*-chlorobenzoate salts (*N*-hydroxyammonium-type salts) of the corresponding amine oxides, whose chemical shifts differ somewhat from those of the free amine oxides. Thus, the chemical shifts we reported in Pohl *et al*.[29] for **5a–9a** are, in reality, the averaged shifts of **5a–9a** and **5b–9b** (for details, refer to the following discussion).

Recently, we have found that the correlation between observed and calculated chemical shifts can be improved when the NMR experiment is performed under specific conditions. First, chemical shifts of amine oxides should be measured in acid-free $CDCl_3$. It is generally known that $CDCl_3$ decomposes by long-term storage producing phosgene and hydrogen chloride. Amine oxides are weak bases (pK_a ~4.5), and upon protonation with strong acids, *N*-hydroxyammonium salts are formed.[30,31] Our measurement of *N*-methylmorpholine *N*-oxide **9a** in common (non-stabilized) $CDCl_3$ at various concentrations (1 M, 100 mM, 10 mM and 1mM) showed significant concentration dependence of the observed chemical shifts. When the same measurement is performed in $CDCl_3$ passed through basic alumina, only slight concentration dependence was observed (Supporting Information, Fig. S1). We have believed that described "concentration dependence" is caused by protonation of *N*-oxide by HCl present in not stabilized $CDCl_3$. Second, ^{13}C chemical shifts should be referenced to TMS. Usually, ^{13}C chemical shifts are referenced to the $CDCl_3$ signal (77 ppm). When we explored the ^{13}C chemical shifts concentration dependence of **9a** even in acid-free $CDCl_3$, we found that the chemical shift of $CDCl_3$ is influenced by *N*-oxide at high (1 M) concentration. Therefore, we recommend to reference ^{13}C chemical shifts of amine oxides to TMS or measure diluted solutions (≤100 mM) of amine oxides when referencing to the $CDCl_3$ signal (Supporting Information, Figs S2 and S3). Third, it is advisable to treat amine oxide, formed by *in situ* oxidation with MCPBA, by addition of Et_3N. Oxidation of tertiary amines with MCPBA produces *m*-chlorobenzoic acid (pK_a = 3.81), which can protonize amine oxides and therefore influence the observed chemical shifts. The effect is illustrated by the ^{13}C NMR spectra of authentic *N*-oxide **9a**, product of the oxidation of amine **9** with MCPBA, and authentic *N*-oxide **9a** after addition of a strong acid [trifluoroacetic acid (TFA), pK_a = 0.23], shown in Fig. 3. It can be seen that each carbon signal of the MCPBA-oxidized product (spectrum b) appears in an intermediate position between those of the pure *N*-oxide (spectrum a) and its TFA-protonized form (spectrum c). That means that the product of MCPBA oxidation of **9** is a fast equilibrium mixture of *N*-oxide **9a** and its corresponding *N*-hydroxyammonium form **9b** as a somewhat prevailing component.

To the best of our knowledge, there is no report describing isolation of *N*-hydroxyammonium *m*-chlorobenzoates or *m*-chloroperbenzoates, although spectral evidence was provided in several cases.[32,33] The improved preparation of amine oxides[34] using MCPBA and treatment with alkaline alumina were described. The method requires chromatography of the reaction mixture on basic alumina with methanol–chloroform elution. To

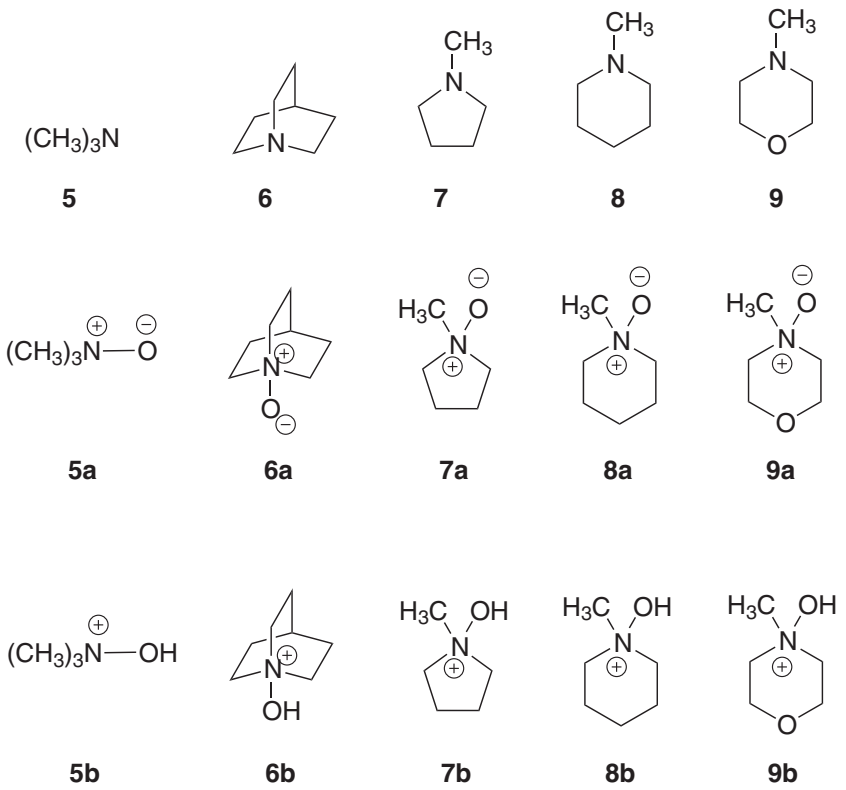

Figure 2. Model amines **5–9**, amine oxides **5a–9a** and their protonized forms **5b–9b**.

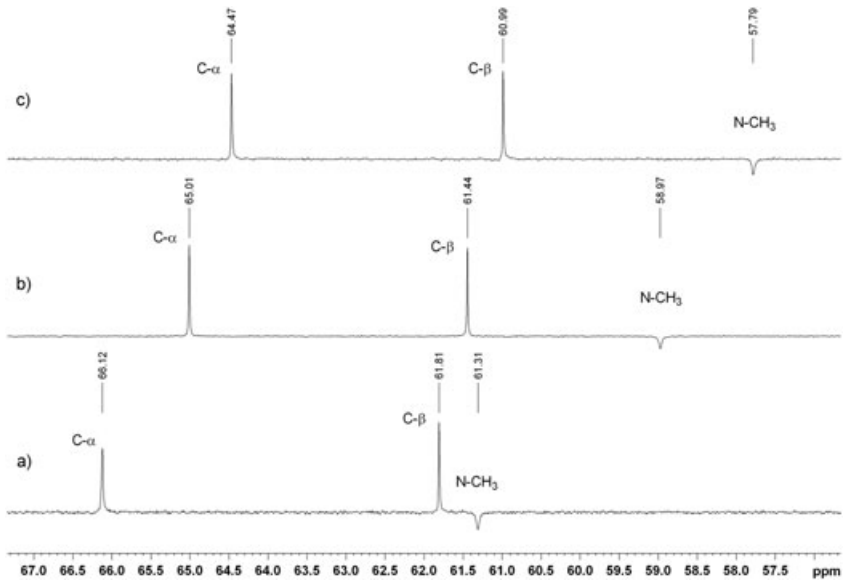

Figure 3. The ^{13}C NMR spectra: (a) authentic *N*-oxide **9a**, (b) product of the oxidation of **9** with MCPBA and (c) authentic *N*-oxide **9a** after addition of TFA.

keep our simple *in situ* concept, we have tested the addition of Et_3N ($pK_a = 10.65$) into NMR tube to destroy *N*-hydroxyammonium *m*-chlorobenzoates formed during oxidation with MCPBA. Using this improved method of *in situ* oxidation by MCPBA with subsequent neutralization of *m*-chlorobenzoic acid, we were able to reproduce experimental ^1H and ^{13}C NMR spectra of the authentic sample of **9a** (Supporting Information, Figs S4 and S5).

With experimental NMR data of model compounds in our hands, we attempted to reproduce them by GIAO DFT calculations. First, we optimized geometry of the molecules using B3LYP/6-31G* method. It is obvious that calculated nuclear shieldings are very sensitive to the geometry of the molecule. Therefore, prior to the NMR data calculation, it is necessary to perform a conformation analysis. The conformation analysis for model compounds **5–9** and **5a–9a** has been already published in our previous paper,[29] and we used the conformations population for the nuclear shielding calculation. There are two possible conformers in the case of protonized *N*-oxides **7b–9b** (*anti* and *gauche*, Fig. 4) that have to be taken into account when calculating NMR parameters. ^{13}C chemical shifts were calculated on the optimized geometries using OPBE/6-31G*, and the results are shown in Table 1. We were pleased to see that such undemanding calculation method provided acceptable reproducibility of experimental values with mean absolute error (MAE) of 1.5 ppm. Apart from this, we were able to distinguish between protonized **5b–10b** and neutral forms **5a–10a** of amine oxides. Experimental ^{13}C data show that, e.g. N–CH_3 group in protonized form is about 1.1–3.8 ppm more shielded compared with neutral amine oxide. The same observation is obvious from calculated ^{13}C data (shielding of CH_3 in range of 3.0–4.1 ppm).

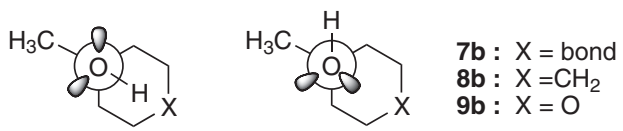

Figure 4. Conformers of *N*-hydroxyammoniums **7b–9b**.

Determination of *N*-oxide configuration of 1-methylpiperidine derivatives

The ^{13}C NMR data of extensive series of saturated azaheterocyclic tertiary amines and corresponding *N*-oxides were recently published.[37,24] We have chosen some of these compounds – five methyl-substituted 1-methylpiperidine derivatives **10–14** and their *N*-oxides **10a–14a** and **10b–14b** as model compounds (Fig. 5) – to check a method for the assignment of *N*-oxide configuration by comparison of calculated and experimental ^{13}C chemical shifts.

The geometries of amines **10–14** and corresponding *N*-oxides **10a–14a** and **10b–14b** were optimized using the DFT B3LYP/6-31G* method, and then ^{13}C chemical shifts were calculated by the GIAO DFT OPBE/6-31G* method. The comparison of the observed and calculated data together with oxidation-induced chemical shifts ($\Delta\delta = \delta_{aminoxide} - \delta_{amine}$) is presented in Fig. 6 and in more detail in the Supporting Information (Tables S5–S9). It can be seen that largest ^{13}C chemical shift difference between epimeric *N*-oxides appear for the N–CH_3 group. The N–CH_3 signal in *N*-oxides with axial N–O bond resonates about 6–13 ppm at higher frequency than in their epimers with equatorial N–O bond in good agreement with calculated differences (5–10 ppm). The carbon atoms in the α-position and β-position show opposite and smaller differences (observed 1.3–3.4 ppm low-frequency shift in axial *N*-oxides and somewhat higher 2.3–7.3 ppm calculated values). It means that ^{13}C chemical shifts calculation/experimental comparison can be used for distinguishing epimeric *N*-oxides and determining *N*-oxide configuration.

Determination of *endo*/*exo* configuration of tropane alkaloids *N*-oxides

Encouraged by the performance of OPBE/6-31G* and B3LYP/6-31G* chemical shift calculation/geometry optimization method, we applied the same strategy to the stereochemical problem – determination of *endo*/*exo* configuration of tropane *N*-oxide derivatives **1a–4a** and **1b–4b**. The conformation of tropane derivatives **1–4** is already known for a long time, and the

Table 1. Comparison of experimental and calculated ^{13}C chemical shifts[a] of model amines **5–9**, amine oxides **5a–9a** and *N*-hydroxyammoniums **5b–9b**

	N–CH_3		C-α		C-β		C-γ	
	Obs.	Calc.	Obs.	Calc.	Obs.	Calc.	Obs.	Calc.
5	47.6	45.0	—	—	—	—	—	—
5a[35]	62.1	60.4	—	—	—	—	—	—
5b[35]	58.3	56.7	—	—	—	—	—	—
6	—	—	47.6	47.8	26.6	27.4	20.6	23.1
6a[36]	—	—	63.5	64.2	27.0	28.5	20.4	22.6
6b		—	61.1	61.5	25.9	27.8	19.7	20.3
7	42.0	40.8	56.2	55.0	24.0	27.0	—	—
7a	55.5	55.0	69.3	68.3	22.1	26.4	—	—
7b	54.4	52.0	68.6	69.0	21.9	24.5	—	—
8	46.7	45.5	56.4	53.0	25.8	26.5	23.7	24.6
8a[24]	59.6	60.5	66.1	64.8	21.1	22.3	21.7	23.3
8b	57.8	56.4	66.4	65.6	20.9	21.9	21.3	20.6
9	46.4	45.2	55.4	51.4	66.9	65.4	—	—
9a[b]	61.3	60.7	66.0	63.5	61.7	61.8	—	—
9b	58.9	56.9	65.0	63.0	61.5	60.7	—	—

[a]OPBE/6-31G*, referenced to TMS calculated at the same level of theory.
[b]Commercial sample of *N*-oxide **9a**.

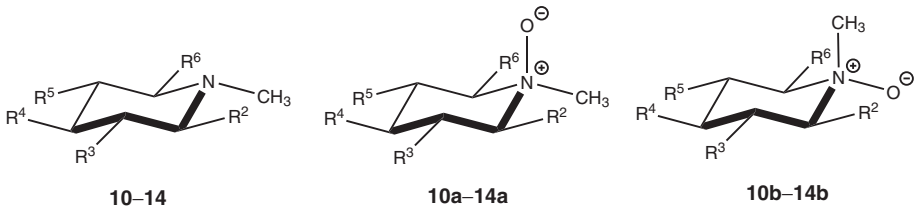

10–14 **10a–14a** **10b–14b**

	R^2	R^3	R^4	R^5	R^6
10, 10a, 10b	Me	H	H	H	H
11, 11a, 11b	H	Me	H	H	H
12, 12a, 12b	H	H	Me	H	H
13, 13a, 13b	Me	H	H	H	Me
14, 14a, 14b	H	Me	H	Me	H

Figure 5. The series of model methyl-substituted 1-methylpiperidine derivatives **10–14** and their *N*-oxides **10a–14a** and **10b–14b**.

conformations shown in Figs 9–12 present the most stable and highly predominant (>99%) conformations found by calculation of ΔG_{298}. We have not taken into account the rotation of methyloxycarbonyl and benzoyloxy group in cocaine. In the case of conformation equilibrium, the calculated chemical shifts were weighted according to the Boltzman distribution of the conformers.

Tropane N-oxides **1a** and **1b**

Tropane **1** was *in situ* oxidized in an NMR tube by MCPBA with subsequent neutralization by Et_3N providing 2:3 mixture of **1a**:**1b** (Fig. 7). Observed ^{1}H and ^{13}C chemical shifts were assigned using NMR experiments described in the experimental part.

In the next step, the geometries of tropane and tropane *N*-oxides were optimized using DFT B3LYP/6-31G* method. The parent amine **1** exists as a mixture of two fast interconverting conformers caused by pyramidal flip on nitrogen atom, which has to be taken into account when calculating NMR parameters. Therefore, geometries of both conformers **1*exo*** and **1*endo*** were optimized, and the ΔG_{298} value was obtained by vibrational analysis (Fig. 8). More stable is the *exo* conformation, with the methyl group in equatorial position. On the other hand, the major product of the oxidation possesses opposite configuration than the more stable conformer **1*exo*** suggesting kinetically controlled reaction. Major *N*-oxide **1b** is formed by an attack from the less-hindered equatorial face.

The optimized geometries of **1*exo***, **1*endo***, **1a** and **1b** were used for calculation of nuclear shielding constants using the GIAO DFT OPBE/6-31G* method. Calculated ^{13}C NMR shifts of **1a** and **1b** and weighted values for **1** according to the Boltzmann distribution of **1*exo*** and **1*endo*** were compared with observed ones, and the results are shown in Fig. 9; a comprehensive table containing both ^{1}H and ^{13}C data can be found in the Supporting Information (Table S1). We have also compared oxidation-induced chemical shifts ($\Delta\delta = \delta_{aminoxide} - \delta_{amine}$) that were successfully used for configuration determination of sulfoxides.[6]

The comparison in Fig. 9 reveals diagnostic carbons useful for stereostructural assignment – carbons directly connected to nitrogen and β carbons influenced by γ-*gauche* and γ-*anti* effects

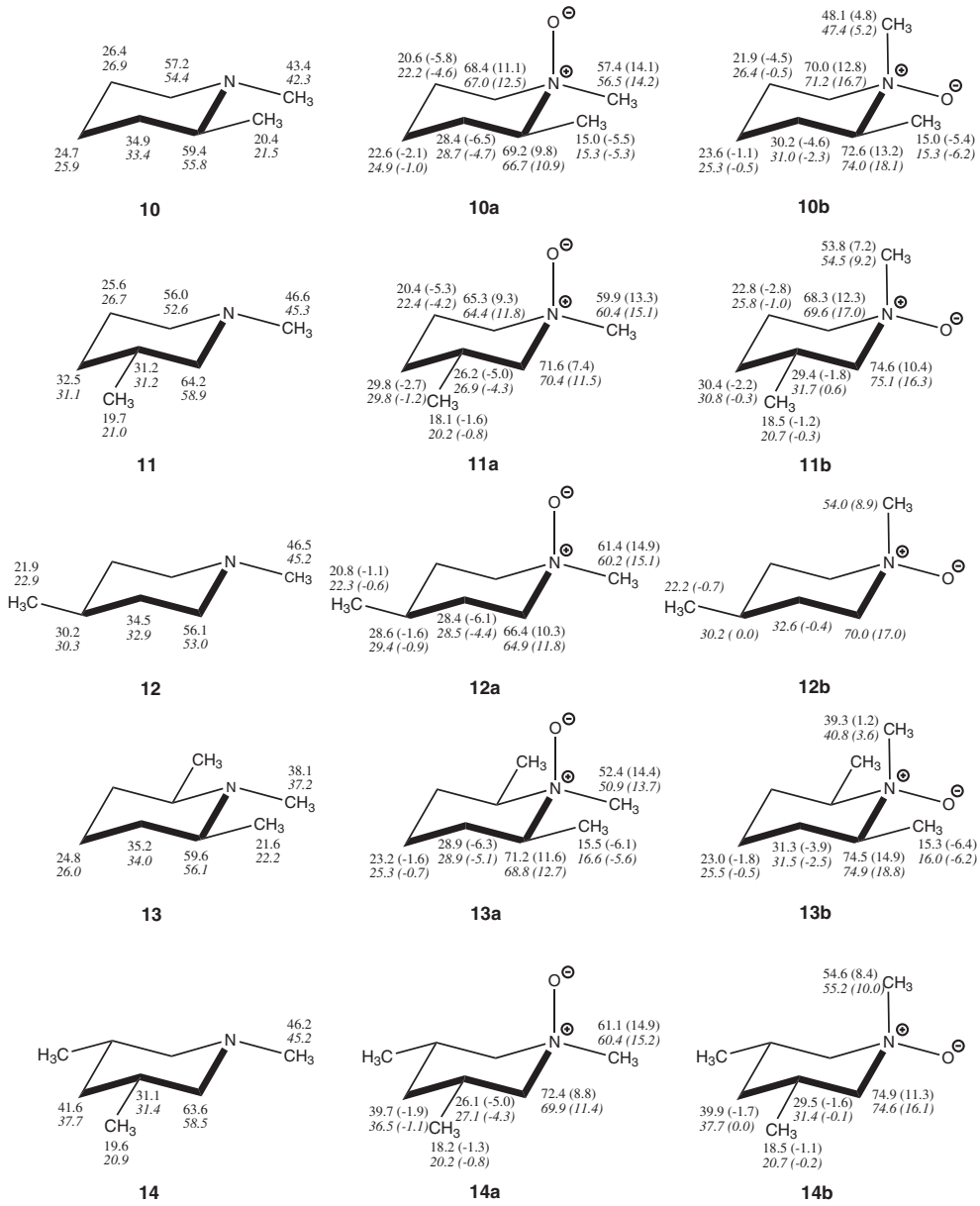

Figure 6. Comparison of observed and calculated (italic) ^{13}C chemical shifts for **10–14**, **10a–14a**, **10b–14b** and corresponding oxidation-induced chemical shifts (in parentheses). Experimental data for **12b** were not obtained.

of N–O and N–CH_3 groups. Thus, in *endo* isomer **1a**, both C-2,4 and C-6,7 are more shielded compared to **1b**. The most sensitive configuration probe is the carbon of the N–CH_3 group. It was postulated[38,39] that the γ-*gauche* effect can be rationalized by changes in bond angles caused by steric interaction. Indeed, a bond angle change influences bonding orbital hybridization, which results in a change in the shielding of the nucleus. As results from DFT optimized geometries, in the case of **1a**, the dihedral angle of H_3C–N–$C_{1,5}$–$C_{6,7}$ is 72° and the distance of H_3C–$HC_{6,7}$ is 2.97 Å. On the other hand, the CH_3N group in **1b** is more influenced by the γ-*gauche* effect because the H_3C–$HC_{2,4}$ distance is 2.73 Å and the dihedral angle of H_3C–N–$C_{1,5}$–$C_{2,4}$ is 55°, and therefore, the carbon atom of the axial N–CH_3 group is more shielded. The observed chemical shift difference of CH_3 for **1a** *versus* **1b** is 7.8 ppm, and the chemical shifts can be predicted by calculation with satisfactory accuracy.

Tropinone N-oxides **2a** and **2b**

Next, we applied the same strategy to other tropane derivatives. Thus, tropinone **2** was *in situ* oxidized in an NMR tube by MCPBA with subsequent neutralization by Et_3N providing 2:3 mixture of **2a**:**2b**. Chemical shifts were then calculated by OPBE/6-31G* method employing B3LYP/6-31G* optimized geometries. The starting amine is a mixture of ***2exo***:***2endo*** 4:5 ($\Delta G_{298} = 0.13$ kcal/mol) according to the B3LYP/6-31G* vibrational analysis. The comparison of observed *versus* calculated ^{13}C chemical shifts is provided in Fig. 10, and a comprehensive table containing both ^{1}H and ^{13}C data can be found in the Supporting Information (Table S2).

Again, chemical shift of CH_3-N carbon was predicted with high accuracy and can be used for unambiguous differentiation between **2a** and **2b**. Also, β carbons, especially C-2,4, showed a good correlation. On the other hand, C-3 was predicted with

Magnetic Resonance in Chemistry

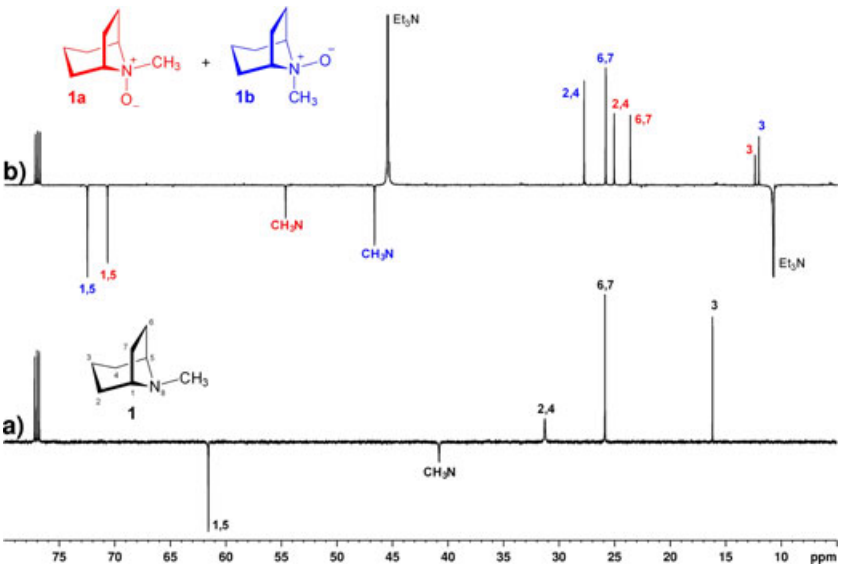

Figure 7. Part of ^{13}C NMR spectrum showing signals of (a) tropane **1** and (b) tropane *N*-oxides **1a** and **1b** after *in situ* oxidation by MCPBA followed by treatment with Et_3N.

the highest error (MAE = 13.9 ppm). The prediction for carbonyl can be improved by addition of polarization and diffuse functions to basis set, and using OPBE/6-311++G** decreases MAE to 3.3 ppm. Because C-3 is not the diagnostic carbon for the configuration determination, we preferred using fast OPBE/6-31G*.

Pseudopelletierine N-oxides **3a** and **3b**

In situ oxidation of pseudopelletierine **3** provided 3:2 mixture of **3a**:**3b** reflecting opposite stereoselectivity of the oxidation compared with **1** and **2**. Optimization and vibrational analysis of starting amine **3** gave an idea about conformation equilibrium between ***3exo***:***3endo*** that was 2:5 (ΔG_{298} = 0.54 kcal/mol).

When we compared the observed and calculated ^{13}C chemical shifts, we found more subtle differences than in the case of **1a**,**1b** and **2a**,**2b** isomers. It is believed that the shielding of the N–CH_3 group in tropane *N*-oxides is caused by γ-gauche and γ-anti effects with C-2,4 and/or C-6,7. Because the nature of the effects in the case of pseudopelletierine *N*-oxides **3a** and **3b** is of the similar magnitude, the chemical shifts of the N–CH_3 group differ less. Nevertheless, it was possible to distinguish between **3a** and **3b** using chemical shifts of CH_3N and β carbons (Fig. 11 and Table S3).

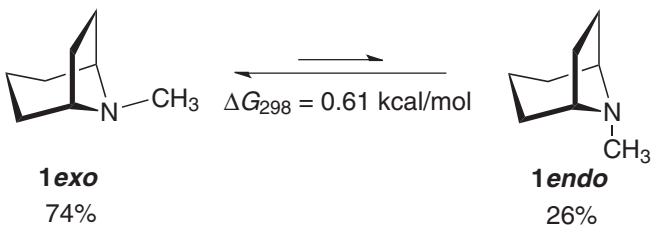

Figure 8. Conformation equilibrium of tropane **1**.

Cocaine N-oxides **4a** and **4b**

Cocaine **4** as an example of chiral tropane derivative was *in situ* oxidized with higher stereoselectivity providing 1:3 mixture of diastereoisomers **4a**:**4b**. Again, conformation equilibrium for **4** was calculated as ***4exo***:***4endo*** 9:1 (ΔG_{298} = 1.34 kcal/mol). Figure 12 shows the comparison of observed and calculated ^{13}C chemical shifts, and complete sets of ^{1}H and ^{13}C data are provided in the Supporting Information (Table S4). Indeed as in previous cases, ^{13}C chemical shifts of CH_3N and β carbons were again proved to be useful for **4a** *versus* **4b** differentiation.

Correlation of experimental and calculated ^{1}H and ^{13}C chemical shifts

In this work, ^{13}C chemical shifts were used for distinguishing axial/equatorial *N*-oxides of 1-methylpiperidine derivatives as model compounds and *endo/exo* isomers of tropane *N*-oxide derivatives. We calculated also ^{1}H chemical shifts, but the correlation with observed values is less satisfactory compared with the ^{13}C nucleus

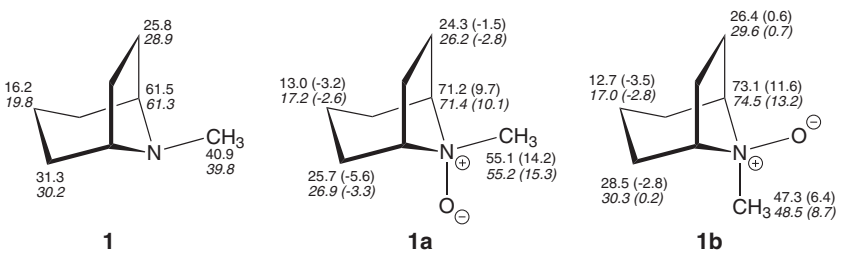

Figure 9. Comparison of observed and calculated (italic) ^{13}C chemical shifts for **1**, **1a**, **1b** and corresponding oxidation-induced chemical shifts (in parentheses).

(Fig. 13). The inferior ^{1}H correlation has been observed earlier[40,29] and could be rationalized by neglecting solvent effect and vibrational averaging.[41] All calculations presented here were performed *in vacuo* because previous calculations[42,43] showed that using the polarizable continuum model for the inclusion of the solvent effect did not improve the results of the calculation.

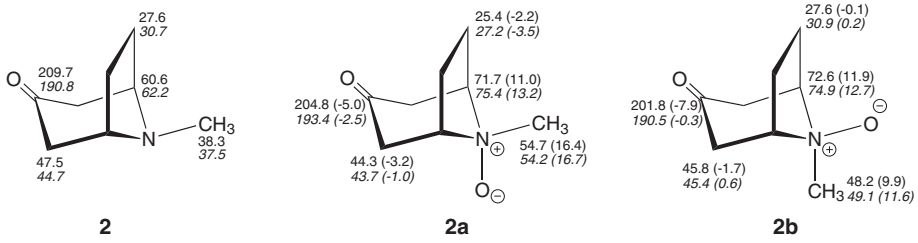

Figure 10. Comparison of observed and calculated (italic) ^{13}C chemical shifts for **2**, **2a**, **2b** and corresponding oxidation-induced chemical shifts (in parentheses).

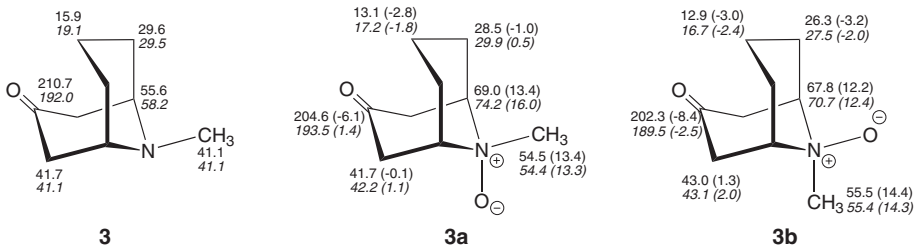

Figure 11. Comparison of observed and calculated (italic) ^{13}C chemical shifts for **3**, **3a**, **3b** and corresponding oxidation-induced chemical shifts (in parentheses).

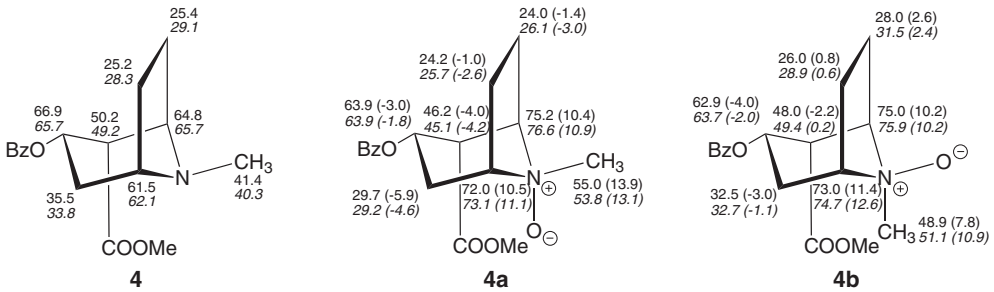

Figure 12. Comparison of observed and calculated (italic) ^{13}C chemical shifts for **4**, **4a**, **4b** and corresponding oxidation-induced chemical shifts (in parentheses).

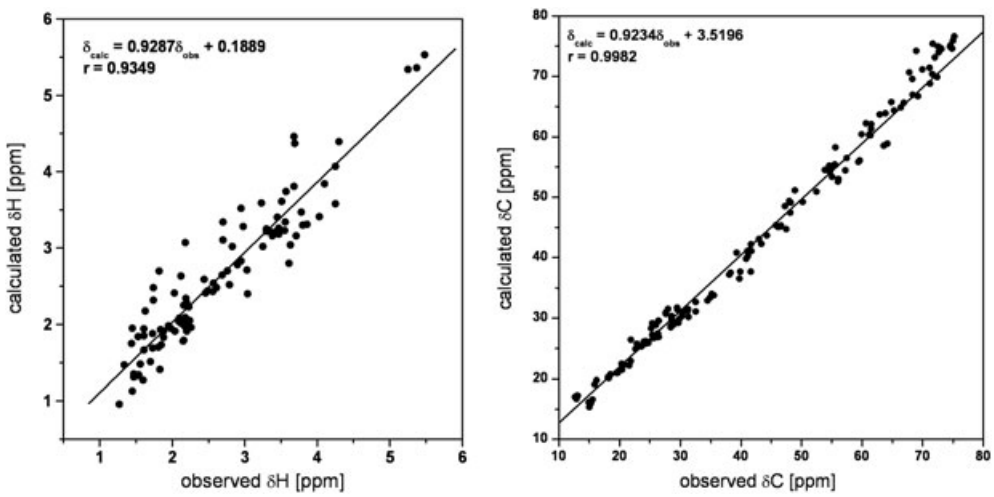

Figure 13. The correlation between calculated and observed ^{1}H chemical shifts in **1–4**, **1a–4a** and **1b–4b** (left) and ^{13}C chemical shifts in **1–4**, **1a–4a**, **1b–4b**, **10–14**, **10a–14a** and **10b–14b** (right, carbonyls included in the correlation but not shown).

Conclusions

In this paper, we described the improved *in situ* method for conversion of tertiary amines to amine oxides on the basis of oxidation by MCPBA and subsequent decomposition of *N*-hydroxyammonium *m*-chlorobenzoates by triethylamine. Observed ^{13}C chemical shifts were correlated with those calculated by OPBE/6-31G* GIAO DFT method. This undemanding calculation method was capable to reproduce experimental values with satisfactory accuracy. We applied this method to distinguish axial/equatorial *N*-oxides of 1-methylpiperidine derivatives as model compounds and to predict *endo/exo* configuration in tropane *N*-oxide derivatives. We found that the experiment/calculation comparison approach can be used for distinguishing epimeric *N*-oxides. The approach enables assigning of the configuration with high degree of certainty even if NMR data of only one isomer are available. The most sensitive configuration probe is the CH_3 group directly connected to the nitrogen ring, and the prediction for this carbon was carried out with MAE of 0.90 ppm.

Acknowledgement

This work was supported by the Czech Science Foundation (grant no. 203/09/1919).

References

[1] D. Neuhaus, M. P. Williamson, *The Nuclear Overhauser Effect in Structural and Conformational Analysis*, Wiley-VCH, New York, USA, **2000**.
[2] M. Karplus. *J. Am. Chem. Soc.* **1963**, *85*, 2870–2871.
[3] C. Thiele, V. Schmidts, B. Bottcher, I. Louzao, R. Berger, A. Maliniak, B. Stevensson. *Angew. Chem. Int. Ed.* **2009**, *48*, 6708–6712.
[4] G. Bifulco, P. Dambruoso, L. Gomez-Paloma, R. Riccio. *Chem. Rev.* **2007**, *107*, 3744–3779.
[5] S. Smith, J. Goodman. *J. Am. Chem. Soc.* **2010**, *132*, 12946–12959.
[6] M. Dračínský, R. Pohl, L. Slavětínská, J. Janků, M. Buděšínský. *Tetrahedron-Asymmetry* **2011**, *22*, 356–366.
[7] A. Shafiee, K. Morteza-Semnani, M. Amini. *J. Nat. Prod.* **1998**, *61*, 1564–1565.
[8] S. Ohmiya, H. Otomasu, J. Haginiwa, I. Murakoshi. *Phytochemistry* **1978**, *17*, 2021–2022.
[9] K. Lim, O. Hiraku, K. Komiyama, T. Koyano, M. Hayashi, T. Kam. *J. Nat. Prod.* **2007**, *70*, 1302–1307.
[10] B. Ma, C. Wu, J. Yang, R. Wang, Y. Kano, D. Yuan. *Helv. Chim. Acta* **2009**, *92*, 1575–1585.
[11] H. Yamaguchi, A. Numata, K. Hokimoto. *Yakugaku Zasshi-J. Pharm. Soc. Jpn.* **1974**, *94*, 1115–1122.
[12] P. Katavic, M. Butler, R. Quinn, P. Forster, G. Guymer. *Phytochemistry* **1999**, *52*, 529–531.
[13] B. Zanolari, D. Guilet, A. Marston, E. Queiroz, M. Paulo, K. Hostettmann. *J. Nat. Prod.* **2005**, *68*, 1153–1158.
[14] Y. Nishiyama, M. Moriyasu, M. Ichimaru, M. Sonoda, K. Iwasa, A. Kato, F. Juma, S. Mathenge, P. Mutiso. *J. Nat. Med.* **2007**, *61*, 56–58.
[15] S. Ott, B. Tofern-Reblin, K. Jenett-Siems, K. Siems, F. Mueller, M. Hilker, B. Onegi, L. Witte, E. Eich. *Z. Naturforsch. B* **2007**, *62*, 285–288.
[16] E. Queiroz, B. Zanolari, A. Marston, D. Guilet, L. Burgener, M. Paulo, K. Hostettmann. *Nat. Prod. Commun.* **2009**, *4*, 1337–1340.
[17] A. Malkov, P. Kočovský. *Eur. J. Org. Chem.* **2007**, 29–36.
[18] I. ONeil, C. Turner, S. Kalindjian. *Synlett* **1997**, 777–780.
[19] G. Caldwell, A. Gauthier, J. Mills, M. Greco. *Magn. Reson. Chem.* **1993**, *31*, 309–317.
[20] G. Caldwell, A. Gauthier, J. Mills. *Magn. Reson. Chem.* **1996**, *34*, 505–511.
[21] V. Křen, J. Němeček, V. Přikrylová. *Coll. Czech. Chem. Commun.* **1995**, *60*, 2165–2169.
[22] S. Pospíšil, P. Sedmera, P. Halada, L. Havlíček, J. Spížek. *Tetrahedron Lett.* **2004**, *45*, 2943–2945.
[23] F. Potmischil, H. Herzog, J. Buddrus. *Magn. Reson. Chem.* **1998**, *36*, 240–244.
[24] F. Potmischil. *Rev. Roum. Chim.* **2006**, *51*, 719–734.
[25] F. Potmischil, H. Duddeck, A. Nicolescu, C. Deleanu. *Magn. Reson. Chem.* **2007**, *45*, 231–235.
[26] F. Potmischil, D. Magiera, H. Duddeck, J. Buddrus. *Magn. Reson. Chem.* **2001**, *39*, 593–599.
[27] M. J. Frisch, G. W. Trucks, H. B. Schlegel, G. E. Scuseria, M. A. Robb, J. R. Cheeseman, G. Scalmani, V. Barone, B. Mennucci, G. A. Petersson, H. Nakatsuji, X. Caricato, X. Li, H. P. Hratchian, A. F. Izmaylov, J. Bloino, G. Zheng, J. L. Sonnenberg, M. Hada, M. Ehara, K. Toyota, R. Fukuda, J. Hasegawa, M. Ishida, T. Nakajima, Y. Honda, O. Kitao, H. Nakai, T. Vreven, J. A. Montgomery, J. E. Peralta, F. Ogliaro, M. Bearpark, J. J. Heyd, E. Brothers, K. N. Kudin, V. N. Staroverov, R. Kobayashi, J. Normand, K. Raghavachari, A. Rendell, J. C. Burant, S. S. Iyengar, J. Tomasi, M. Cossi, N. Rega, J. M. Millam, M. Klene, J. E. Knox, J. B. Cross, V. Bakken, C. Adamo, J. Jaramillo, R. Gomperts, R. E. Stratmann, O. Yazyev, A. J. Austin, R. Cammi, C. Pomelli, J. W. Ochterski, R. L. Martin, K. Morokuma, V. G. Zakrzewski, G. A. Voth, P. Salvador, J. J. Dannenberg, S. Dapprich, A. D. Daniels, O. Farkas, J. B. Foresman, J. V. Ortiz, J. Cioslowski, D. J. Fox, *Gaussian 09*, Gaussian, Inc., Wallingford CT, **2009**.
[28] Y. Zhang, A. Wu, X. Xu, Y. Yan. *Y. Chem. Phys. Lett.* **2006**, *421*, 383–388.
[29] R. Pohl, M. Dračínský, L. Slavětínská, M. Buděšínský. *M. Magn. Reson. Chem.* **2011**, *49*, 320–327.
[30] Y. Shvo, E. D. Kaufman. *J. Org. Chem.* **1982**, *47*, 2190–2192.
[31] H. Volz, H. Gartner. *Eur. J. Org. Chem.* **2007**, 2791–2801.
[32] F. Potmischil, V. Cîmpeanu, O. Cuza. *Rev. Chim.(Bucureşti)* **2004**, *55*, 351–355.
[33] M. Palucki, P. Pospisil, W. Zhang, E. Jacobsen. *J. Am. Chem. Soc.* **1994**, *116*, 9333–9334.
[34] J. C. Craig, K. K. Purushothaman. *J. Org. Chem.* **1970**, *35*, 1721–1722.
[35] G. Olah, D. Donovan, H. Lin, H. Mayr, P. Andreozzi, G. Kloopman. *J. Org. Chem.* **1978**, *43*, 2268–2272.
[36] I. O'Neil, I. Bhamra. *Tetrahedron Lett.* **2009**, *50*, 3635–3638.
[37] F. Potmischil, V. Cîmpeanu, H. Herzog, J. Buddrus, H. Duddeck. *Magn. Reson. Chem.* **2003**, *41*, 554–556.
[38] E. Kleinpeter, P. Seidl. *J. Phys. Org. Chem.* **2004**, *17*, 680–685.
[39] D. Wilton, R. Kitahara, K. Akasaka, M. Williamson. *J. Biomol. NMR* **2009**, *44*, 25–33.
[40] M. Dračínský, R. Pohl, L. Slavětínská, M. Buděšínský. *Magn. Reson. Chem.* **2010**, *48*, 718–726.
[41] M. Dračínský, J. Kaminský, P. Bouř. *J. Chem. Phys.* **2009**, *130*, 094106.
[42] M. Dračínský, P. Bouř. *J. Chem. Theory Comput.* **2010**, *6*, 288–299.
[43] M. Dračínský, J. Kaminský, P. Bouř. *J. Phys. Chem. B* **2009**, *113*, 14698–14707.